

Crystallographic Analysis of Drug and Inhibitor-Binding Structure of RND-Type Multidrug Exporter AcrB in Physiologically Relevant Asymmetric Crystals

Ryosuke Nakashima, Keisuke Sakurai, and Akihito Yamaguchi

Abstract

Xenobiotic extruding pumps have recently been known to be widely distributed in living organisms from mammalian to bacteria as a host-defense mechanism in cellular level. These pumps not only confer multidrug resistance of cancer cells and pathogenic bacteria but also cause hereditary diseases through the mutation. Our purposes are to elucidate the molecular structures and mechanisms of these xenobiotic exporters.

We had succeeded to determine the crystal structure of bacterial major multidrug exporter AcrB at 3.5 Å resolution (Murakami et al., *Nature* 419:587–593, 2002) and elucidated the structural bases of substrate recognition that the pump recognize the places and thus act as a “membrane vacuum cleaner.” After that we also determined the crystal structure of the drug-binding form of AcrB in space group *C*2 in which asymmetric unit contains structurally asymmetric homo-trimer of AcrB (Murakami et al., *Nature* 443:173–179, 2006; Nakashima et al., *Nature* 480:565–569, 2011; Nakashima et al., *Nature* 500:120–126, 2013). Analyses revealed the existence of a specific mechanism to recognize numerous substrates that the multisite binding is the base of multidrug recognition rather than induced-fit, and functional-rotation mechanism in which three monomers undergo a strictly coordinated sequential conformational change cycle of access, binding, and extrusion. Determination of physiological asymmetric AcrB structure was crucially important to understand these transport mechanisms.

Key words Multidrug exporter AcrB, RND family, Crystallization, X-ray, Crystal structure, Functional-rotation mechanism, Peristaltic pump mechanism

1 Introduction

AcrB and its homologues are the major multidrug transporters in Gram-negative bacteria and play important role in drug resistance. AcrB, the resistance-nodulation-cell division (RND) transporter, is a homotrimer that acts as a tripartite complex with the multifunctional outer membrane channel, TolC and the membrane fusion protein (MFP), AcrA. This complex is constitutively expressed in

bacterial cells and is responsible for the natural resistance against toxic compounds like dyes, detergents, and antibiotics.

In spite of the relative abundance of AcrB in nature, it is still difficult to get the protein in high amount and in crystallization compatible quality from a natural source. Therefore we used bacterial recombinant expression system. It must contribute to reducing future labor to optimize protein expression condition in advance of purification/crystallization trials. We inspected combination of some types of plasmid, host strains, broth, induction (timing, concentration of the inducer, incubation time) and found that, in the case of AcrB, when pACBH and JM109 was used as expression vector and host, respectively, protein expression level became maximum. In this chapter, we introduce the actual situation from bacterial culture to crystallographic analysis of AcrB.

2 Materials

All solutions were prepared with ultrapure water (Milli-Q Integral 3) and guaranteed or higher-grade reagent.

2.1 Expression

1. His-tagged and tag-free AcrB was inserted in pUC118 vector, and *E. coli* bacteria strain JM109 was transformed with these AcrB-containing plasmids.
2. Medium A [1]: 17.5 g K_2HPO_4 , 7.5 g KH_2PO_4 , 1.25 g Na_3 citrate·3H₂O, 0.25 g $MgSO_4$ ·7H₂O, 2.5 g $(NH_4)_2SO_4$ in a final volume of 2.5 L.
3. 20% (w/v) glucose and 10% (w/v) casamino acids were sterilized separately with Medium A to avoid Maillard reaction.
4. Bacterium cultivation was performed with Bioshaker BR-3000LF (TAITEC Corp., Japan) at 37 °C and 180 rpm. It has the ability to load eight flasks of 5 L.

2.2 Purification

1. CR22 high-speed refrigerated centrifuge with R18C continuous flow rotor (Hitachi Koki, Ltd.) was used to harvest bacteria.
2. Buffer A: 50 mM Tris-HCl pH 7.0, 10% (v/v) glycerol, 1 mM $MgCl_2$, 0.5 mM EDTA.
3. Buffer B: 5 mM Tris-HCl pH 7.0, 0.5 mM EDTA.
4. Buffer C: 50 mM Tris-HCl pH 7.0, 10% (v/v) glycerol.
5. Bacterial lysis was performed with laboratory homogenizer APV 1000 (SPX Corporation) at 4 °C and 950 bar.
6. Sucrose Monododecanoate (Dodecanoyl sucrose/DDS) was purchased from Affymetrix (former Anatrace).

7. Iminodiacetic acid sepharose beads (IDA) for immobilized metal ion affinity chromatography were purchased from GE healthcare (Chelating Sepharose™ Fast Flow). It can be immobilized various metal ions such as Cu^{2+} , Zn^{2+} , Ni^{2+} , and Fe^{3+} . Among them, Ni^{2+} ion was immobilized.
8. Column chromatography was performed with 12 ml Econo-column (Bio-Rad).
9. Buffer D: 20 mM Tris-HCl pH 7.5, 10% (v/v) glycerol, 300 mM NaCl, 0.1% (w/v) DDS.
10. Buffer E: 20 mM Tris-HCl pH 7.5, 10% (v/v) glycerol, 300 mM NaCl, 0.1% (w/v) DDS, 25 mM Imidazole-HCl pH 7.5.
11. Buffer F: 20 mM Tris-HCl pH 7.5, 10% (v/v) glycerol, 300 mM NaCl, 0.1% (w/v) DDS, 100 mM Imidazole-HCl pH 7.5.
12. Buffer G: 20 mM Tris-HCl pH 7.5, 10% (v/v) glycerol, 300 mM NaCl, 0.1% (w/v) DDS, 300 mM Imidazole-HCl pH 7.5.
13. Amicon-stirred cell (Model 8010, Merck Millipore) and Bio-max Ultrafiltration membrane (NMWL: 100 kDa, Merck Millipore) was used to concentrate protein.
14. Buffer H: 20 mM Sodium phosphate pH 6.2, 10% (v/v) glycerol, 0.1% (w/v) DDS.
15. BCA assay was used to determine protein concentration. BSA was used as a protein standard.
16. Buffer I: 20 mM Tris-HCl pH 7.5, 10% (v/v) glycerol, 0.1% (w/v) DDS.
17. Buffer J: 20 mM Tris-HCl pH 7.5, 10% (v/v) glycerol, 0.1% (w/v) DDS, 300 mM NaCl.
18. n-Dodecyl β -D-maltoside was from GLYCON Biochemicals (Germany).
19. Q sepharose HP was from GE healthcare.

2.3 Crystallization

1. Polyethylene Glycol 4000 and 400 were purchased from Hampton Research.
2. CrystalClear D Strips was from Hampton Research.
3. Buffer K: 100 mM Sodium phosphate pH 6.2, 100 mM NaCl, 12% (w/v) Polyethylene Glycol 4000.
4. Buffer L: 100 mM Sodium phosphate pH 6.2, 100 mM NaCl, 14% (w/v) Polyethylene Glycol 4000.
5. Buffer M: 60 mM Sodium phosphate pH 6.2, 50 mM NaCl, 5% (w/v) glycerol, 0.1% (w/v) DDS, 10% (w/v) PEG4000.

6. Buffer N: 60 mM Sodium phosphate pH 6.2, 50 mM NaCl, 30% (w/v) glycerol, 0.1% (w/v) DDS, 11% (w/v) PEG4000.
7. LithoLoops (Protein Wave Corp., Japan) was used for crystal mounting.

3 Methods

Carry out all procedures at 4 °C (in cold chamber or ice bath) unless otherwise specified.

3.1 Bacterial Membrane Preparation

1. The plasmid encoding his-tagged AcrB is previously constructed [2]. The cloned chromosomal *acr* locus from *E. coli* W3104 was inserted into pUC118 vector (pAC8), followed by addition of a (His)₄ sequence at the 3' end of the *acrB* gene (pACBH). Since AcrB has intrinsic His-His sequence at its C-terminal, the resulting AcrB protein has six histidine tag. This plasmid contains *acrR*, *acrA*, *acrB*, and their promoter region, and hence it expresses encoding proteins without induction.
2. *E. coli* strain JM109 harboring pACBH was cultured in 2xYT broth containing 100 µg/ml ampicillin at 37 °C until OD₆₀₀ reaches 0.7–1.0, and then cell cultures were diluted into 100-fold volume of minimal medium (Medium A) (*see Note 1*) supplemented with 0.2% (w/v) glucose and 0.1% (w/v) casamino acids and cultured more 7 h at 37 °C (*see Note 2*). Incubation was performed in 5 L Erlenmeyer flask in bioshaker with rotating mode. Cultivation of 30 L in total was carried out with two shakers and 12 flasks (*see Note 3*).
3. The cells were collected by centrifugation at 24,000 × *g* with R18C continuous flow rotor at 4 °C. 80 g wet cells are usually obtained from 30 L culture.
4. The cells were suspended in buffer A at 5 ml/g wet cell and disrupted with laboratory homogenizer APV 1000 at 950 bar.
5. After elimination of debris by several high-speed centrifugation, membrane fractions were collected by ultracentrifugation at 158,000 × *g* for 90 min. The resulting precipitate was suspended with buffer B to wash out membrane-associated proteins and then ultracentrifuged again. The purified membrane fractions were suspended in buffer C and divided into approximately 200 mg protein/tube. And then they were frozen in liquid nitrogen and stored at –80 °C until further protein purification.

3.2 Protein Purification (Six Histidine-Tagged AcrB)

1. The protocol used to purify AcrB is previously described in [3]. The membrane fraction was thawed and adjusted to 10 mg/ml protein, then it was solubilized by adding 20% DDS solution quickly to become 1.5% (w/v) of final concentration while mixing it.

2. After 20 min gently stirring, the solubilized membrane fraction was centrifuged for 1 h at $172,000 \times g$, and the supernatant was applied to a 5 ml Ni Sepharose resin pre-equilibrated with buffer D with batch mode.
3. After incubation for 1 h, resin was collected into a column, and proteins were purified by column chromatography. The resin was washed with 10 column volume each of buffer E and F.
4. The proteins were eluted with 10 column volume of buffer G.
5. Buffer composition of eluate was exchanged into buffer H by three successive concentration–dilution steps using an Amicon-stirred cell with 100 kDa cutoff ultrafiltration membrane, which was pressurized with five nines nitrogen gas, and proteins were finally concentrated to approximately 35 mg/ml (see **Notes 4** and **5**). About 12 mg highly purified proteins as shown in Fig. 1 are usually obtained at once. Purified AcrB can be cryopreserved but preferable are immediately submitted to crystallization set up.
6. Protein concentration was determined using BCA assay.

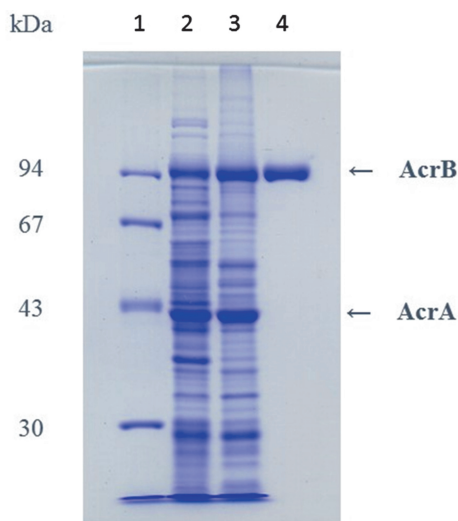


Fig. 1 Analysis of protein purification by SDS-PAGE. Proteins were separated by 10% PAGE and stained by Coomassie Brilliant Blue. *Lane 1*: Molecular maker (LMW, GE Healthcare), *lane 2*: whole cell, *lane 3*: membrane fraction, *lane 4*: purified AcrB. 30% (w/v) Acrylamide/Bis Mixed Solution (37.5:1) was used to prepare a 1 mm thick, 10% gel based on Laemli method (8 cm \times 19 cm \times 0.1 cm wide gel, Seema-biotech Co., Ltd., Japan). Sample buffer in reductive condition was used to prepare loading samples. Loading samples were not boiled to avoid AcrB aggregation. Electrophoresis was performed at 45 mA constant current. The gels were stained with 0.1% (w/v) CBB R-250/40% ethanol/10% acetic acid for 30 min and destained until a background disappeared in 40% ethanol/10% acetic acid

3.3 Protein Purification (Tagless AcrB)

1. The method of cultivation and membrane preparation are same as that of His-tagged AcrB except for using bacteria harboring pAC8.
2. Membrane fraction was solubilized by 2.0% (w/v) DDS. After incubation for 20 min, it was centrifuged for 1 h at $172,000 \times g$, and then the resulting supernatant was applied to a 5 ml Q sepharose HP resin pre-equilibrated with buffer I with batch mode.
3. After 1 h incubation, resin was collected into a column, and proteins were purified afterwards by column chromatography. The column was washed with 10 column volume of equilibration buffer I.
4. The proteins were eluted with a linear gradient (100 ml total volume) of buffer I and J.
5. Fractions containing AcrB judged from electrophoresis were pooled and was applied directly (without buffer exchange) to a 5 ml Ni Sepharose resin pre-equilibrated with buffer K with batch mode again. Since AcrB has intrinsic His-His sequence at its C-terminal as described above, native AcrB trimer has six histidine tags in total. For this reason, Ni affinity chromatography is available. But this feature of AcrB often causes the problem that it is easy to contaminate in the preparation of histidine tag fusion proteins [4].
6. After 1 h incubation, resin was collected into a column and was washed with 10 column volume of buffer E.
7. The proteins were eluted with 10 column volume of buffer F. It is the same as histidine-tagged AcrB afterward.

3.4 Crystallization of Native AcrB

1. Native Crystals of AcrB were prepared as previously described [3]. Crystals were grown at 25 °C using the sitting drop vapor diffusion method. Protein solution of 28 mg/ml in buffer H was mixed with equal volume of reservoir solution which was a mixture of buffer K and L. 4 μ l crystallization drops were setup in the CrystalClear D Strips and sealed with microplate sealer.
2. For the crystallization of space group C2 in which the asymmetric unit contains AcrB trimer, the microseeding method was used to induce crystallization (*see Note 6*). A tungsten needle was used to dislodge seeds from a crystal. The needle was touched to all crystallization drop surface to promote crystal growth from the drop surface (Fig. 2a) before strips were sealed. The crystals came to be visible within few hours. The crystals were harvested after growing up 1 week (*see Note 7*).

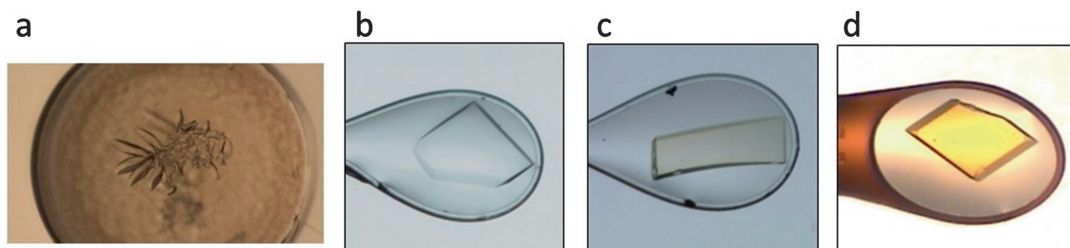


Fig. 2 Photographs of AcrB C2 crystal. (a) A photograph of sitting drop, (b) native (drug-free), (c) minocycline complex, (d) rifampicin complex

3.5 Crystallization of AcrB-Drug (Inhibitor) Complex

3.5.1 In Case of Hydrophilic Compounds

1. The crystallization condition of drug complex was the same as native crystal except for containing drug at molar ratio of 3–50. The drugs were dissolved in buffer H necessary to dilute protein solution to 28 mg/ml. To ensure AcrB–drug complex formation, substrate was added to the purified protein and incubated for a few hours at 4 °C prior to crystallization set up.
2. Microseeding was also performed in drug complex crystallization same as native crystallization in which native crystal was used as seed.

3.5.2 In Case of Hydrophobic Compounds

1. Before buffer exchange of protein fraction using amicon, substrates that were dissolved in ethanol or DMSO were added to eluate from a Ni-column at approximately tenfold of molar ratio with the protein. After incubation of several hours, the solvent was washed out with buffer exchange by three concentration–dilution steps (*see Note 8*).
2. The substrate concentration in the final protein sample can be determined by either spectroscopic measurement or by LC–MS/MS for quantitative analysis [5].
3. Microseeding was also performed in drug complex crystallization same as native crystallization.

3.6 Cryo Protection

1. Cryoprotection was achieved by raising the glycerol concentration stepwise to 30% (v/v) (buffer N) in 5% increments, and each step took 10 min (*see Notes 9 and 10*). Crystals were picked using LithoLoops for flash cooling in a cold nitrogen gas stream (100 K) from a cryostat (*see Note 11*). In most cases of AcrB, it would function as a crystal harvesting buffer if the concentration of precipitant is raised a little in comparison to initial condition when crystallization drop was set up (buffer M). For drug complex crystal, drug was also contained in crystal harvesting buffer.

3.7 Characterization: SAXS (Small Angle X-ray Scattering)

1. Protein sample for crystallization was used in the SAXS measurement. Dispersion curves of protein in each protein concentration were obtained by circular averaging of measurement images with the program SAXSGui and background reduction with Primus (ATSAS). The concentration-dependent multimer formation was not observed.
2. Inertial radius and Dmax value calculated by the program Gnom (ATSAS) using the data in the range up to $q = 0.67 \text{ \AA}^{-1}$ were 79.46 and 208.0 Å, respectively.
3. Dummy Residues Model (DRM) was built using Gasbor (ATSAS). The solution structure was obtained by averaging four results of Gasbor (Fig. 3). This result revealed that the protein forms a dimer (MexB trimer $\times 2$) in solution. Although this is the result measured with MexB sample not AcrB sample, we think it is almost identical to that of AcrB because the AcrB/DDS sample includes great amount of an ingredient to elute in a void volume of size exclusion chromatography using Superdex 200 10/300 GL (*see Note 12*).

3.8 Crystallographic Analysis

1. Each data set was collected using the BL44XU beamline at SPring-8 with an MX225-HE charge-coupled-device detector (Rayonix) at 100 K.
2. The diffraction data were processed and scaled using the HKL2000 [6] package or MosFlm in the CCP4 program suite [7].
3. The initial phases were first determined by molecular replacement with MOLREP [8] using the atomic coordinates of AcrB (Protein Data Bank ID, 2DHH) as a search model.

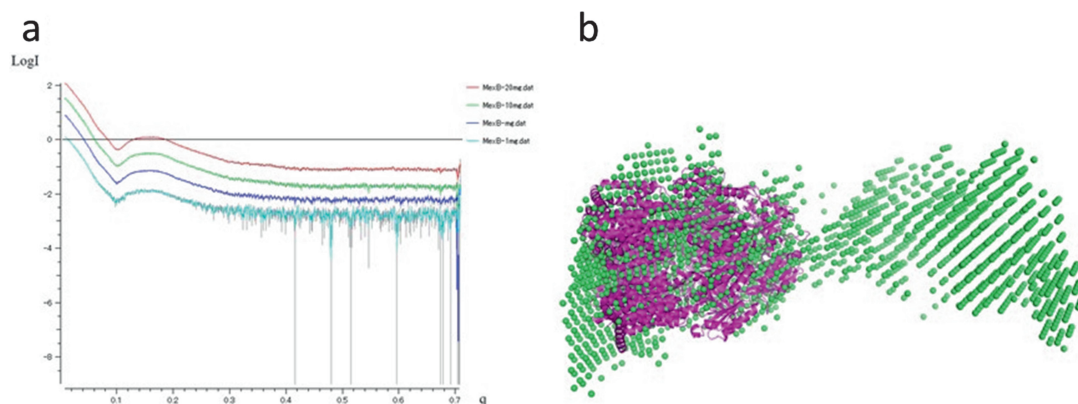


Fig. 3 Solution structure of RND pump in dimer of trimmers. (a) A dispersion curves of protein in each concentration, (b) the solution structure calculated using Gasbor. MexB trimer (*magenta*) was superimposed onto solution structure (*green*). Measuring conditions were as follows: X-ray Generator/Camera: FR-E+/BioSAXS-1000 (Rigaku Corp.), Camera length: 500 mm, Sample condition: MexB, range of 20–0.1 mg/ml (10 mM Tris–HCl pH 7.5, 50 mM NaCl, 0.05% DDM), sample volume: 30 μ l, Room temperature

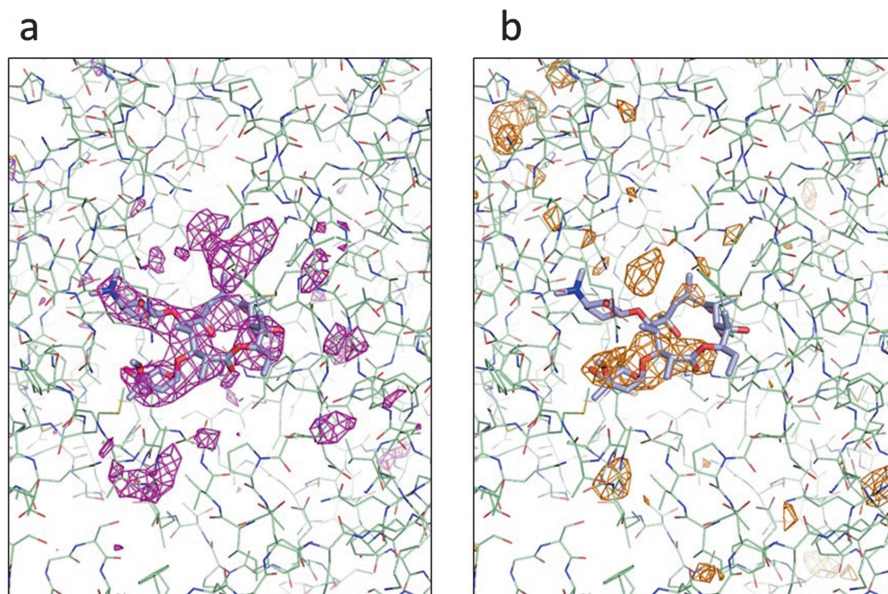


Fig. 4 Comparison of initial $F_{O(\text{liganded})} - F_{O(\text{unliganded})}$ and $F_o - F_c$ electron density maps for the region of erythromycin binding site. Protein moiety and erythromycin are drawn in wire model and gray stick model, respectively. (a) $F_{O(\text{liganded})} - F_{O(\text{unliganded})}$ map contoured at 3σ is shown in *magenta*, (b) $F_o - F_c$ map contoured at 3σ is shown in *orange*. We calculated maps after molecular replacement (Molrep) and refinement (restrained refinement with Refmac5). Suitable solution was provided when the initial map was calculated with the differences between the observed structure factors as coefficient. Because $F_o - F_o$ map requires that the isomorphism being kept between the crystals and substrate-free crystal exist, this method is not applicable to the proteins of which substrate-free crystal is not available like MexB

4. Model rebuilding was performed using COOT [9], and model refinement was performed using CNS [10] and REFMAC [11].
5. To identify drug molecules in the AcrB–drug complexed crystals, different Fourier electron density maps were calculated with coefficients of $(|F_{O(\text{liganded})}| - |F_{O(\text{unliganded})}|) \exp(i\alpha_{\text{unliganded}})$, where $F_{O(\text{liganded})}$ is the structure factor in the presence of a bound drug, $F_{O(\text{unliganded})}$ is the structure factor of the drug-free crystal, and $\alpha_{\text{unliganded}}$ is the phase of the drug-free crystal (Fig. 4). Refinement was performed with constrained structures for the drug molecules.

4 Notes

1. Because the RND family has the tendency that protein expression level was low in rich broth like 2xYT, the minimal medium was used for protein expression.

2. Bacterial cells were harvested within 7 h from a main culture start because bacteriolysis was observed in the stationary phase of pACBH/JM109 cultivation.
3. For unknown reasons, protein expression level was also low in large scale cultivation in 50 L or larger Jar fermentor. Then we limited culture scale up to 2.5 L in flask.
4. The protein sample changes its solubility after size exclusion chromatography, probably because the number of phospholipid remaining in final protein sample was reduced. However, it was not adopted as protein purification step because it didn't improve the quality of the crystal.
5. Although detergent was concentrated with increasing protein concentration, excessive detergent composition pass into the filtrate because micelle size of DDS was below the membrane molecular weight cut-off. For this reason, there is no necessary to treat concentrated protein solution by Bio-Beads to remove excess detergent.
6. Because crystallization condition of the space group C2 produced many protein precipitate, seeding that induced crystal growth from drop surface (Fig. 2a) was necessary to obtain good crystals. When the concentration of precipitant and/or protein were reduced, it resulted in a small crystal.
7. Although the crystal grew up for one month and reached the maximum size of up to 1 mm, there was considerable decrease in crystal quality after growing. In consideration of size and quality, crystals were harvested within 7–10 days.
8. The method of Subheading 3.5.2 has the problem that it is difficult to control drug concentration. However, it is necessary to remove the organic solvent because it usually has bad effect on crystallization.
9. At first, the cryoprotectant should be chosen among the components of mother liquor. In case of AcrB C2 crystal, glycerol was chosen [2] and in case of MexB, PEG400 was raised as protectant [5]. If these reagents that work as cryoprotectants are not included in mother liquor, I will test glycerol, low molecular weight PEG like PEG200 and 400, ethylene glycol, and so on.
10. A crystal cracks when the cryo-protection process is hurried, and a crystal changes in quality into sponge state without appearances change when it is soaked against the solution of high concentration glycerol for more than a day. Therefore the processing by dialysis to be seen elsewhere is not applicable to AcrB C2 crystal. It seems to be sufficient spending 10 min on each step.

11. In case of AcrB C2 crystal, cryostream was used to freeze crystal instead of liquid nitrogen. When crystal was soaked into liquid nitrogen directly, the isomorphism (it is important for analysis of substrate-binding structure) was lost, and ability to diffract X-ray was also decreased. On the other hand in case of a crystal of other homolog, we know that the direct method has better results. It is not decided which method is superior, therefore it is necessary to test both stream and direct method at first.
12. There are many reports on crystal structure of RND-type transporter including symmetric {AcrB [3, 12–16], AcrB/YajC [17], AcrB/AcrZ [18], CusA [19], CusAB [20], MtrD [21]}, and asymmetric {AcrB [22, 23, 24], AcrB/DARPin [25], MexB [5, 26], ZneA [27]} trimer. The symmetric structure is regarded as resting form, while the asymmetric structure is regarded as physiologically relevant structure and is essential to elucidate the mechanism of RND transporter. Because RND-type transporters have a pseud threefold symmetry axis at the center of the trimer, it might have a tendency to crystallize easily into the space group having crystallographic threefold symmetry. Therefore we think that using the protein binder such as DARPin and the dimer of trimer formation are effective to obtain the physiologically relevant asymmetric crystals.

Acknowledgements

This work was supported by CREST, JST.

References

1. McMurphy L, Petrucci RE Jr, Levy SB (1980) Active efflux of tetracycline encoded by four genetically different tetracycline resistance determinants in *Escherichia coli*. *Proc Natl Acad Sci U S A* 77:3974–3977
2. Fujihira E, Tamura N, Yamaguchi A (2002) Membrane topology of a multidrug efflux transporter, AcrB, in *Escherichia coli*. *J Biochem (Tokyo)* 131:145–151
3. Murakami S, Nakashima R, Yamashita E, Yamaguchi A (2002) Crystal structure of bacterial multidrug efflux transporter AcrB. *Nature* 419:587–593
4. Veesler D, Blangy S, Cambillau C, Sciara G (2008) There is a baby in the bath water: AcrB contamination is a major problem in membrane-protein crystallization. *Acta Crystallogr Sect F Struct Biol Cryst Commun* 64:880–885
5. Nakashima R, Sakurai K, Yamasaki S, Hayashi K, Nagata C, Hoshino K, Onodera Y, Nishino K, Yamaguchi A (2013) Structural basis for the inhibition of bacterial multidrug exporters. *Nature* 500:120–126
6. Otwinowski Z, Minor W (1997) Processing of X-ray diffraction data collected in oscillation mode. *Methods Enzymol* 276:307–326
7. Collaborative Computational Project (1994) Number 4. The CCP4 suite: programs for protein crystallography. *Acta Crystallogr D* 50:760–763
8. Vagin A, Teplyakov A (1997) MOLREP: an automated program for molecular replacement. *J Appl Crystallogr* 30:1022–1025

9. Emsley P, Cowtan K (2004) Coot: model-building tools for molecular graphics. *Acta Crystallogr D* 60:2126–2132
10. Brunger AT (2007) Version 1.2 of the crystallography and NMR system. *Nat Protoc* 2:2728–2733
11. Murshudov GN, Vagin AA, Dodson EJ (1997) Refinement of macromolecular structures by the maximum-likelihood method. *Acta Crystallogr D* 53:240–255
12. Yu EW, McDermott G, Zgurskaya HI, Nikaido H, Koshland DE Jr (2003) Structural basis of multiple drug binding capacity of the AcrB multidrug efflux pump. *Science* 300:976–980
13. Pos KM, Schiefner A, Seeger MA, Diederichs K (2004) Crystallographic analysis of AcrB. *FEBS Lett* 564:333–339
14. Das D, Xu QS, Lee JY, Ankoudinova I, Huang C, Lou Y, DeGiovanni A, Kim R, Kim SH (2007) Crystal structure of the multidrug efflux transporter AcrB at 3.1 Å resolution reveals the N-terminal region with conserved amino acids. *J Struct Biol* 158:494–502
15. Drew D, Klepsch MM, Newstead S, Flaig R, De Gier JW, Iwata S, Beis K (2008) The structure of the efflux pump AcrB in complex with bile acid. *Mol Membr Biol* 25:677–682
16. Hung LW, Kim HB, Murakami S, Gupta G, Kim CY, Terwilliger TC (2013) Crystal structure of AcrB complexed with linezolid at 3.5 Å resolution. *J Struct Funct Genom* 14:71–75
17. Törnroth-Horsefield S, Gourdon P, Horsefield R, Brive L, Yamamoto N, Mori H, Snijder A, Neutze R (2007) Crystal structure of AcrB in complex with a single transmembrane subunit reveals another twist. *Structure* 15:1663–1673
18. Du D, Wang Z, James NR, Voss JE, Klimont E, Ohene-Agyei T, Venter H, Chiu W, Luisi BF (2014) Structure of the AcrAB-TolC multidrug efflux pump. *Nature* 509:512–515
19. Long F, Su CC, Zimmermann MT, Boyken SE, Rajashankar KR, Jernigan RL, Yu EW (2010) Crystal structures of the CusA efflux pump suggest methionine-mediated metal transport. *Nature* 467:484–488
20. Su CC, Long F, Zimmermann MT, Rajashankar KR, Jernigan RL, Yu EW (2011) Crystal structure of the CusBA heavy-metal efflux complex of *Escherichia coli*. *Nature* 470:558–562
21. Lei HT, Chou TH, Su CC, Bolla JR, Kumar N, Radhakrishnan A, Long F, Delmar JA, Do SV, Rajashankar KR, Shafer WM, Yu EW (2015) Crystal structure of the *Neisseria gonorrhoeae* MtrD inner membrane multidrug efflux pump. *PLoS One* 6:e97475
22. Murakami S, Nakashima R, Yamashita E, Matsumoto T, Yamaguchi A (2006) Crystal structures of a multidrug transporter reveal a functionally rotating mechanism. *Nature* 443:173–179
23. Seeger MA, Schiefner A, Eicher T, Verrey F, Diederichs K, Pos KM (2006) Structural asymmetry of AcrB trimer suggests a peristaltic pump mechanism. *Science* 313:1295–1298
24. Sennhauser G, Amstutz P, Briand C, Storchenegger O, Grütter MG (2006) Drug export pathway of multidrug exporter AcrB revealed by Darpin inhibitors. *PLoS Biol* 5:e7
25. Sennhauser G, Bukowska MA, Briand C, Grütter MG (2009) Crystal structure of the multidrug exporter MexB from *Pseudomonas aeruginosa*. *J Mol Biol* 389:134–145
26. Pak JE, Ekendé EN, Kifle EG, O'Connell JD 3rd, De Angelis F, Tessema MB, Derfoufi KM, Robles-Colmenares Y, Robbins RA, Goormaghtigh E, Vandenbussche G, Stroud RM (2013) Structures of intermediate transport states of ZneA, a Zn(II)/proton antiporter. *Proc Natl Acad Sci U S A* 110:18484–18489
27. Nakashima R, Sakurai K, Yamasaki S, Nishino K, Yamaguchi A (2011) Structures of the multidrug exporter AcrB reveal a proximal multisite drug-binding pocket. *Nature* 480:565–569

Bacterial Multidrug Exporters

Methods and Protocols

Yamaguchi, A.; Nishino, K. (Eds.)

2018, XII, 355 p. 91 illus., 53 illus. in color., Hardcover

ISBN: 978-1-4939-7452-8

A product of Humana Press